

# Magnetism in parent Fe-chalcogenides: quantum fluctuations select a plaquette order

Samuel Ducatman, Natalia B. Perkins, Andrey Chubukov<sup>1</sup>

<sup>1</sup>*Department of Physics, University of Wisconsin-Madison, Madison, WI 53706, USA*

(Dated: today)

We analyze magnetic order in iron-chalcogenide  $\text{Fe}_{1+y}\text{Te}$  – the parent compound of high-temperature superconductor  $\text{Fe}_{1+y}\text{Te}_{1-x}\text{Se}_x$ . Neutron scattering experiments show that magnetic order in this material contains components with momentum  $Q_1 = (\pi/2, \pi/2)$  and  $Q_2 = (\pi/2, -\pi/2)$  in Fe-only Brillouin zone. The actual spin order depends on the interplay between these two components. Previous works argued that spin order is a single- $Q$  state (either  $Q_1$  or  $Q_2$ ). Such an order breaks rotational  $C_4$  symmetry and order spins into a double diagonal stripe. We show that quantum fluctuations actually select another order – a double  $Q$  plaquette state with equal weight of  $Q_1$  and  $Q_2$  components, which preserves  $C_4$  symmetry but breaks  $Z_4$  translational symmetry. We argue that the plaquette state is consistent with recent neutron scattering experiments on  $\text{Fe}_{1+y}\text{Te}$ .

*Introduction.* The analysis of magnetism in parent compounds of iron-based superconductors (FeSCs) is an integral part of the program to understand the origin of superconductivity in these materials [1–12]. Parent compounds of Fe-pnictides are moderately correlated metals, whose resistivity increases with increasing  $T$ , and the electronic structure is at least qualitatively consistent with that of free electrons on a lattice [5, 13]. Magnetic order in such systems can be reasonably well understood within itinerant scenario [7–9, 14] due to enhancement of free-electron susceptibility at momenta connecting hole and electron Fermi surfaces (FSs). The locations of the FSs select two possible momenta for the order –  $(0, \pi)$  and  $(\pi, 0)$  – in the Fe-only Brillouin zone (BZ). Electron-electron interaction and the shape of the FSs further reduce the ground state manifold to single-momentum states with either  $(0, \pi)$  or  $(\pi, 0)$ , but not their mixture [9]. In each of these two states spins are ordered in a stripe fashion – ferromagnetically along one direction in 2D Fe-plane and antiferromagnetically in the other. Such an order breaks  $C_4$  lattice rotational symmetry and causes pre-emptive spin-nematic order [15]. The same magnetic order is selected in the strong coupling approach, which assumes that the system is not far from Mott transition, and magnetic properties are reasonably well described by  $J_1 - J_2$  model with nearest and second-nearest neighbor spin exchange [16, 17]. The actual coupling in Fe-pnictides is neither truly small nor strong enough to cause Mott insulating behavior [13], which makes it extremely useful that the two descriptions agree. Upon doping, long-range order is lost, but magnetic fluctuations evolve smoothly and remain peaked at or near  $(0, \pi)$  and  $(\pi, 0)$  even beyond optimal doping [18].

There is one family of FeSCs – 11 Fe-chalcogenides  $\text{Fe}_{1+y}\text{Te}_{1-x}\text{Se}_x$ , in which smooth evolution between parent and optimally doped compounds does not hold. Magnetism in these materials changes considerably between  $x = 0$  and  $x \sim 0.5$ , where the  $T_c$  is the largest. Near optimal doping magnetic fluctuations are peaked at or near  $(0, \pi)$  and  $(\pi, 0)$ , as in Fe-pnictides, while mag-

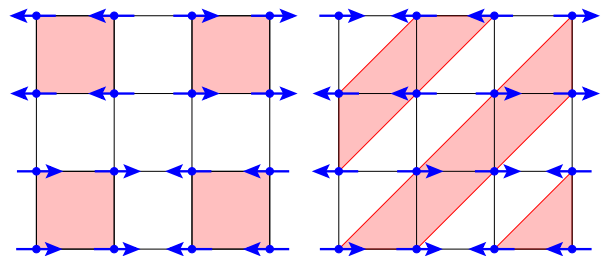


FIG. 1: The two possible collinear configurations for the  $J_1 - J_2 - J_3$  model: (a) orthogonal double stripe (ODS) and (b) diagonal double stripe (DDS).

netic order in a parent compound  $\text{Fe}_{1+y}\text{Te}$  has very different momenta  $\pm(\pi/2, \pm\pi/2)$  [19–23]. Upon doping, the spectral weight at  $\pm(\pi/2, \pm\pi/2)$  decreases, and the spectral weight at  $(0, \pi)$  and  $(\pi, 0)$  increases [20]. The transport properties of  $\text{Fe}_{1+y}\text{Te}$  are also quite different from those of parent compounds of Fe-pnictides: the resistivity,  $\rho(T)$ , of  $\text{Fe}_{1+y}\text{Te}$  does not show a prominent increase with increasing  $T$ , but instead remains flat and even shows a small increase as  $T$  decreases [24]. ARPES studies of  $\text{Fe}_{1+y}\text{Te}$  show that low-energy spectra are very broad [25], consistent with the notion that electrons are not propagating. These observations lead several groups to suggest that parent Fe-chalcogenides are more correlated than parent Fe-pnictides, and magnetism in  $\text{Fe}_{1+y}\text{Te}$  can be understood by assuming that electrons are “almost” localized and interact magnetically via a Heisenberg exchange [26–29]. This scenario is in line with a more generic idea [30–32] that in any FeSc, a certain percentage of electronic states are localized and phase separated from itinerant electrons, and the percentage of localized states varies between different materials. An alternative scenario for FeTe, which we don’t discuss here, is orbital order [33]

In this communication we apply the localized electron scenario to  $\text{Fe}_{1+y}\text{Te}$  and verify whether the observed commensurate  $\pm(\pi/2, \pm\pi/2)$  order can be obtained in a Heisenberg model with exchange interactions up to third

neighbors. Classically,  $\pm(\pi/2, \pm\pi/2)$  order is unstable with respect to a spiral order for any non-zero first neighbor exchange, unless one artificially breaks  $C_4$  symmetry and sets interactions to be spatially anisotropic [21, 30]. We analyze the isotropic quantum Heisenberg model and show that quantum fluctuations do stabilize a commensurate  $\pm(\pi/2, \pm\pi/2)$  order in some range of parameters. However, this stabilization does not uniquely determine spin configuration as a generic  $\pm(\pi/2, \pm\pi/2)$  order is a superposition of two different  $Q$ -vectors:  $\mathbf{Q}_1 = (\pi/2, -\pi/2)$ , and  $\mathbf{Q}_2 = (\pi/2, \pi/2)$ :  $\mathbf{S}(\mathbf{r}) = \Delta_1 \cos \mathbf{Q}_1 \mathbf{r} + \Delta_1' \sin \mathbf{Q}_1 \mathbf{r} + \Delta_2 \cos \mathbf{Q}_2 \mathbf{r} + \Delta_2' \sin \mathbf{Q}_2 \mathbf{r}$ , with  $|\Delta_i| = |\Delta_i'| = \Delta$  and  $\Delta_1 \cdot \Delta_2 = \Delta_1' \cdot \Delta_2' = 0$ . In Fig. 1 we show two prototypical commensurate spin configurations – a single  $Q$  bi-collinear spin order ( $\Delta_1 = \Delta_1' = \Delta$ ,  $\Delta_2 = \Delta_2' = 0$ ), which breaks  $C_4$ , and a double  $Q$  plaquette order ( $\Delta_1 = \Delta_2 = \Delta$ ,  $\Delta_1' = \Delta_2' = 0$ ), which preserves  $C_4$  symmetry, but breaks  $Z_4$  translational symmetry (four equivalent plaquette states are obtained by moving a black square in Fig. 1a by one lattice site in either  $x$  or  $y$  direction). Bi-collinear spin order is often called diagonal double stripe (DDS), and plaquette order is called orthogonal double stripe (ODS), and we use these notations below. The real-space configuration for both orders is “up-up-down-down” along  $x$  and  $y$  directions.

Most of previous theoretical and experimental works assumed that the commensurate order is DDS [10] and studied in detail the feedback from this order on electrons [21]. We argue that quantum fluctuations of spins actually select ODS order as a stable collinear state for weak but finite nearest-neighbor exchange  $J_1$ , while DDS state is unstable for any non-zero  $J_1$ . The DDS and the ODS orders have qualitatively different forms of the static structure factor  $S(q)$  (two peaks vs four peaks), but this is difficult to detect in real materials because of domains. The authors of [22] however argued that form of  $S(q)$  in a paramagnetic phase allows one to distinguish between DDS and ODS, even in the presence of domains, and found that their results are consistent with strong ODS fluctuations. Another argument in favor of the  $C_4$  preserving ODS spin order is the absence of orthogonal distortion in  $\text{Fe}_{1+y}\text{Te}$  – there is a monoclinic distortion below  $T_N$ , but this does not break rotational in-plane  $C_4$  symmetry. There is also numerical evidence – ODS order has been found in exact diagonalization studies of  $J_1 - J_2 - J_3$  model on clusters up to 36 spins [34]. The same ODS order has been found in the mean-field studies of the  $t - J$  model in another Fe-chalcogenide  $\text{K}_{0.8}\text{Fe}_{1.6}\text{Se}_2$  [35].

*Model.* We follow earlier works and model magnetic interactions in  $\text{Fe}_{1+y}\text{Te}$  by a  $J_1 - J_2 - J_3$  Heisenberg model [27, 28, 34, 36]:

$$H = \sum_{n=1}^3 J_n \sum_{\langle ij \rangle} \vec{S}_i \cdot \vec{S}_{i+n} \quad (1)$$

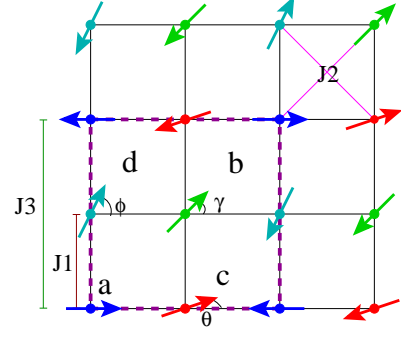


FIG. 2: Spin order in the classical  $J_1 - J_2 - J_3$  model at  $J_1 = 0$ . Classically degenerate configurations form four sublattices, labeled as  $a, b, c$ , and  $d$ . A configuration with arbitrary  $\gamma, \theta$ , and  $\phi$  is a ground state. In our notations, sublattice spins are  $\Delta_1 + \Delta_2$ ,  $\Delta_1 - \Delta_2$ ,  $\Delta_1' - \Delta_2'$ , and  $\Delta_1' + \Delta_2'$ , respectively.

where  $J_1, J_2$ , and  $J_3$  are antiferromagnetic exchange couplings between first-, second-, and third-nearest neighbors. For  $\text{Fe}_{1+y}\text{Te}$  the values of  $J_1, J_2$ , and  $J_3$  have been estimated in [27] and found to be in the range  $J_3 > \frac{J_2}{2} \gg J_1$ . In this limit, the classical ground state of (1) is a spiral with the pitch vector  $\mathbf{Q} = (\pm q, \pm q)$ , where  $q = \arccos(\frac{-J_1}{2J_2+4J_3})$  [37]. At  $J_1 = 0$ , the model has an extensive degeneracy, and any order with momentum  $\pm(\pi/2, \pm\pi/2)$  is the classical ground state, including DDS, ODS, and an infinite number of other four-sublattice states (Fig. 2).

We consider here what happens in the quantum model, at a finite  $J_1$ . We show that the ODS state is unambiguously selected by quantum fluctuations to be the ground state in some range of  $J_1$ , before a spiral order sets in. Our key reasoning is that only some classically degenerate ground states at  $J_1 = 0$  are degenerate by symmetry; others are “accidentally degenerate”. The situation is quite similar to the one in the well-known  $J_1 - J_2$  model at  $J_2 > J_1/2$  [38]. We argue that quantum fluctuations lift accidental degeneracies and gap out some of the spin-wave modes which in the classical limit become unstable (imaginary) at  $J_1 \neq 0$ . For the DDS state the lifting of the accidental degeneracies does not help, as the modes which become unstable at a finite  $J_1$  are the true Goldstone modes at  $J_1 = 0$ . On the other hand, for ODS state classically unstable modes are accidental zero modes at  $J_1 = 0$ , and quantum fluctuations lift the energies of these modes to finite values, making ODS the state stable in a finite range of  $J_1$ . We verified that ODS state is indeed the ground state in this range.

*Large- $S$  spin-wave calculations.* We consider large value of spin  $S$  and study the role of quantum fluctuations within  $1/S$  expansion. The computational steps are presented in [39]. For  $J_1 = 0$ , spins on even and odd sites form two non-interacting sublattices, each described by  $J_2 - J_3$  model. This model is identical to “ $J_1 - J_2$ ” model, with diagonal hopping  $J_2$  playing the role of “ $J_1$ ”

and third-neighbor hopping  $J_3$  playing the role of " $J_2$ ". One can use this analogy and borrow the results of the quantum analysis of " $J_1 - J_2$ " model [38]. For  $J_3 > J_2/2$  (which holds in  $\text{Fe}_{1+y}\text{Te}$ ), quantum fluctuations select stripe configurations within each sublattice, i.e. the angle  $\gamma$  in Fig.2 is locked at  $\gamma = 0$  or  $\gamma = \pi$ , and the angle  $\theta$  is locked at  $\theta = \phi$  or  $\theta = \pi + \phi$ . The states with  $\gamma = 0$  and  $\gamma = \pi$  are equivalent up to an interchange of  $X$  and  $Y$  directions, and below we set  $\gamma = 0$ . The collinear DDS and ODS states belong to the manifold of selected states and correspond to different locking of the angle  $\phi$  between the nearest-neighbor spins: DDS state corresponds to  $\phi = 0, \theta = \pi$  or  $\phi = \pi, \theta = 0$ , while ODS corresponds to  $\phi = \theta = 0$  or  $\phi = \theta = \pi$ .

To analyze whether a generic state selected by quantum fluctuations at  $J_1 = 0$  remains stable at a finite value of  $J_1$ , we need to know its excitation spectrum. At  $J_1 = 0$ , spins on even and odd sites are decoupled, each sublattice is described by its own bose field ( $\alpha_{\mathbf{k}}$  for even sites and  $\beta_{\mathbf{k}}$  for odd sites), and spin-wave excitations are described by

$$H_{sw} = S(\Omega_{\alpha\mathbf{k}}\alpha_{\mathbf{k}}^\dagger\alpha_{\mathbf{k}} + \Omega_{\beta\mathbf{k}}\beta_{\mathbf{k}}^\dagger\beta_{\mathbf{k}}), \quad (2)$$

The classical spin-wave spectrum is the same for all selected states

$$\begin{aligned} \Omega_{\mathbf{k}} &= S(A_{\mathbf{k}}^2 - B_{\mathbf{k}}^2)^{1/2}, \quad A_{\mathbf{k}} = 4J_3 + 2J_2 \cos(k_x + k_y), \\ B_{\mathbf{k}} &= 2J_2(\cos 2k_x + \cos 2k_y) + 2J_2 \cos(k_x - k_y). \end{aligned} \quad (3)$$

This spectrum contains nodes at  $\pm(\pi/2, \pm\pi/2)$ , but some of them are not symmetry-related and are lifted by quantum fluctuations. For the sublattice made of even sites, the order has momentum  $\pm(\pi/2, -\pi/2)$  (Fig. 2 b), hence the true nodes are located only at these momenta, while the ones at  $\pm(\pi/2, \pi/2)$  must be lifted. For the sublattice made out of spins at odd sites, the order has momentum  $\pm(\pi/2, \pi/2)$  if we take  $\theta = \phi$ , like in the ODS, and  $\pm(\pi/2, -\pi/2)$  if we take  $\theta = \pi + \phi$ , like in the DDS. Quantum fluctuations then must lift the nodes at  $\pm(\pi/2, -\pi/2)$  and at  $\pm(\pi/2, \pi/2)$  for the ODS and the DDS state, respectively. We computed quantum corrections to the spectrum in Eq. (3) within perturbation theory to order  $1/S$  and indeed found that accidental nodes are lifted by quantum fluctuations and only true Goldstone modes remain [39].

We next set  $J_1$  to be small but finite and consider which of stripe states, if any, remain stable. The qualitative reasoning is the following: a non-zero  $J_1$  couples the two sublattices and adds to the Hamiltonian (2) the terms in the form  $\alpha_{\mathbf{k}}^\dagger\beta_{\mathbf{k}}$  and  $\alpha_{\mathbf{k}}\beta_{\mathbf{k}}$ . For the DDS state (or, more accurately, for the DDS family of states as we keep  $\phi$  as a parameter) the stripes on even and odd sites are directed parallel to each other, and the dispersions of  $\alpha_{\mathbf{k}}$  and  $\beta_{\mathbf{k}}$  fields are identical, including  $O(1/S)$  terms. The two dispersions are then gapless at the same momenta

$\mathbf{k} = \pm(\pi/2, -\pi/2)$ . Around these  $\mathbf{k}$  points, the perturbation theory in  $J_1$  is singular, as there is no symmetry requirement which would force the coupling to vanish at  $\pm(\pi/2, -\pi/2)$ . As a result, the excitations become purely imaginary close enough to  $\pm(\pi/2, -\pi/2)$ , which implies that the DDS states are unstable at any non-zero  $J_1$ . On the other hand, for the ODS family of states, the dispersions  $\Omega_{\mathbf{k}}^\alpha$  and  $\Omega_{\mathbf{k}}^\beta$  have nodes at different momenta,  $\pm(\pi/2, -\pi/2)$  and  $\pm(\pi/2, \pi/2)$ , respectively. Because of this disparity, perturbation theory near either  $\pm(\pi/2, -\pi/2)$  or  $\pm(\pi/2, \pi/2)$  is not singular, and corrections in  $J_1$  only gradually shift the values of spin-wave velocities thus keeping ODS states stable.

We verified this reasoning by explicit calculations. We first obtained the  $J_1$ -induced interaction in terms of the original Holstein-Primakoff bosons and then re-expressed it in terms of  $\alpha_{\mathbf{k}}$  and  $\beta_{\mathbf{k}}$  bosons from Eq. (2), which are related to the original ones by Bogoliubov transformation. The  $u_{\mathbf{k}}v_{\mathbf{k}}$ -coefficients of this transformation dress up the interaction terms. For the DDS states, expanding the Hamiltonian near the true Goldstone points at  $(\pi/2, -\pi/2)$  as  $\mathbf{k} = (\pi/2, -\pi/2) + \tilde{\mathbf{k}}$  we obtain  $H_{DDS} = H_{sw} + \delta H_{DDS}$ , where  $H_{sw}$  is given by (2) with

$$\Omega_{\mathbf{k}}^\alpha = \Omega_{\mathbf{k}}^\beta \approx 4S\sqrt{J_3(2J_3 + J_2)}(\tilde{k}_x^2 + \tilde{k}_y^2 - 2a\tilde{k}_x\tilde{k}_y)^{1/2}, \quad (4)$$

where  $a = \frac{J_2}{2J_3} < 1$ , and

$$\delta H_{DDS} = \Delta^{DDS}\tilde{\mathbf{k}}(\alpha_{\mathbf{k}}^\dagger\beta_{\tilde{\mathbf{k}}} + \alpha_{\tilde{\mathbf{k}}}\beta_{-\mathbf{k}} + h.c) \quad (5)$$

where

$$\Delta_{\mathbf{k}}^{DDS} = \frac{J_1 S}{2} \left( \frac{2J_3 + J_2}{J_3} \right)^{1/2} \frac{\tilde{k}_y - \tilde{k}_x}{(\tilde{k}_x^2 + \tilde{k}_y^2 - 2a\tilde{k}_x\tilde{k}_y)^{1/2}} \quad (6)$$

The coupling term remains finite when  $\tilde{k}_{x,y}$  tends to zero, except for special directions. Diagonalizing (5) we find that at low enough  $\tilde{k}$  one of the two solutions is  $E_{\tilde{\mathbf{k}}}^2 \approx -2\Omega_{\mathbf{k}}^{\alpha(\beta)}\Delta_{\mathbf{k}}^{DDS}$ . A negative  $E_{\tilde{\mathbf{k}}}^2$  implies that fluctuations around a DDS state grow exponentially with time and make this family of states unstable.

For the ODS states the situation is different because near any of the points  $\pm(\pi/2, -\pi/2)$  or  $\pm(\pi/2, \pi/2)$ , the zero in one of the spin-wave branches is lifted by quantum fluctuations. For example, near  $(-\pi/2, \pi/2)$  expanding of the Hamiltonian again gives  $H_{ODS} = H_{sw} + \delta H_{ODS}$ , however now only  $\Omega_{\mathbf{k}}^\alpha$  is gapless, while  $\Omega_{\mathbf{k}}^\beta$  is gapped with the gap of the order  $1/S$ . The interaction term  $\delta H_{ODS}$  has the same form as in (5), but with

$$\Delta_{\mathbf{k}}^{ODS} = 2J_1 S^2 (2J_3 + J_2) \frac{\tilde{k}_y - \tilde{k}_x}{(\Omega_{\mathbf{k}}^\alpha \Omega_{\mathbf{k}}^\beta)^{1/2}} = O\left(J_1 S^{3/2} |\tilde{\mathbf{k}}|^{1/2}\right). \quad (7)$$

Diagonalizing  $H_{ODS}$  we find two solutions,

$$\begin{aligned} E_{1,2}^2 &= \frac{1}{2} \left( (\Omega_{\tilde{\mathbf{k}}}^\alpha)^2 + (\Omega_{\tilde{\mathbf{k}}}^\beta)^2 \right. \\ &\quad \left. \pm \sqrt{((\Omega_{\tilde{\mathbf{k}}}^\alpha)^2 - (\Omega_{\tilde{\mathbf{k}}}^\beta)^2)^2 + 16(\Delta_{\tilde{\mathbf{k}}}^{ODS})^2 \Omega_{\tilde{\mathbf{k}}}^\alpha \Omega_{\tilde{\mathbf{k}}}^\beta} \right). \end{aligned} \quad (8)$$

One of the solutions is gapped to order  $1/S$ , the other is linear in  $\tilde{k}$  with a stiffness which differs from its value at  $J_1 = 0$  by  $O(J_1 S/J_3)$ . We see that the ODS states are stable (for any  $\phi$ ) as long as  $J_1 S/J_3$  is small.

On a more careful look, we find that the ODS spin order allows for  $J_1$ -induced umklapp processes, which also renormalize the dispersions of the ODS states. Indeed, because ODS state breaks  $Z_4$  translational symmetry, the  $J_1$  interaction contains not only the terms at zero transferred momentum, as in (5), but also terms with momentum transfer in multiples of  $\pi$  along each axis. Near  $k = (\pi/2, -\pi/2)$ , the most relevant of such umklapp terms is the one with momentum  $\tilde{Q} = (0, \pi)$ , which connects a gapless  $\alpha_{\tilde{k}}$  boson at  $(\pi/2, -\pi/2)$ , and a gapless  $\beta_{\tilde{k}}$  boson at  $(\pi/2, \pi/2)$ . However, because breaking of  $Z_4$  is equivalent to breaking local inversion symmetry (a reflection around one column or one row in Fig. 1a), the umklapp vertices  $\Delta_{\tilde{k}}^{U,ODS}$  contain extra momentum gradient compared to non-umklapp vertices. In explicit form, we find at small  $\tilde{\mathbf{k}} = \mathbf{k} - (\pi/2, -\pi/2)$ ,

$$\Delta_{\tilde{\mathbf{k}}}^{U,ODS} = -i \frac{J_1}{4} \left( \frac{\Omega_{\tilde{k}}^\alpha \Omega_{\tilde{k}+\tilde{Q}}^\beta}{4J_3^2 - J_2^2} \right)^{1/2} \cos \phi, \quad (9)$$

where  $\Omega_{\tilde{k}}^\alpha, \Omega_{\tilde{k}+\tilde{Q}}^\beta = 4S(J_3(2J_3 \pm J_2))^{1/2}(\tilde{k}_x^2 + \tilde{k}_y^2 \mp 2\tilde{k}_x\tilde{k}_y)^{1/2}$  and the angle  $\phi$  specifies the spin order within the ODS family of states. We see that  $\Delta_{\tilde{\mathbf{k}}}^{U,ODS}$  scales linearly with  $\tilde{\mathbf{k}}$ , i.e., is of the same order as  $\Omega_{\tilde{k}}^{\alpha\beta}$ . We computed the corrections to spin-wave velocity and found that they scale as  $J_1/\sqrt{4J_3^2 - J_2^2}$ , i.e., are small. At the same time, we see from the Eq.(9) that  $\Delta_{\tilde{\mathbf{k}}}^{U,ODS}$  depends on the angle  $\phi$ . Respectively, the corrections to the ground state energy also depend on  $\phi$  and should select which state within the ODS family has the lowest energy. The computation is straightforward and yields  $\Delta E_{gr} = -A \cos^2 \phi$ , with  $A > 0$ . We see that the collinear ODS state, for which  $\phi = 0$  or  $\pi$ , is indeed the state with the lowest energy.

The outcome of our analysis is that the collinear ODS state remains stable and has the lowest energy within a family of similar states. At small  $J_1$ , the ODS state has a finite stiffness towards fluctuations which tend to break collinear order in favor of a spiral one. The ODS state remains stable up to  $J_1 \sim J_3/S$ , at larger  $J_1$  the stiffness changes sign, and the system develops a spiral order.

*Experimental signatures of ODS state.* Because the ODS state does not break  $C_4$  translational symmetry, it does not cause a pre-emptive spin-nematic order, in contrast to parent compounds of other FeSCs [15]. The data for  $\text{Fe}_{1+y}\text{Te}$  show that the system develops a monoclinic distortion below a certain  $T$ , but in-plane  $C_4$  symmetry remains unbroken (it only breaks in doped compounds  $\text{Fe}_{1+y}\text{Te}_{1-x}\text{Se}_x$  with  $x > 0.5$  [24]). The unbroken  $C_4$  symmetry in the ordered state also manifests itself in

the  $C_4$  symmetry of the static structure factor  $S(q)$  obtained in neutron scattering experiments [22]. We computed  $S(q)$  for both the DDS and the ODS states, and we indeed found that the structure factor for the ODS order has four identical peaks at  $(\pm\pi/2, \pm\pi/2)$ , while the structure factor for the DDS state has only two peaks at  $(\pi/2, -\pi/2)$  and  $(-\pi/2, \pi/2)$ . While the observed four peaks are consistent with ODS, we caution that the absence of the anisotropy in the structure factor obtained in neutron scattering could be due to the twinning of the crystal. However, as the magnetic domain's structure of the crystal can be controlled using polarized neutrons, the careful analysis of the neutron scattering data might dissect the contribution from different domains. The authors of Ref. [22] made another argument that, even in a twinned crystal, the form of  $S(q)$  throughout the Brillouin zone differentiates between strong DDS and ODS fluctuations, and argued that their data are more consistent with tendency towards ODS order. This again agrees with our results.

*Summary.* In this communication we analyzed the type of magnetic order in  $\text{Fe}_{1+y}\text{Te}$  – the parent compound in a family of Fe-chalcogenide superconductors. The magnetic order in this material is different from in other parent compounds of FeSCs – spins are ordered in up-up-down-down fashion (Fig. 2). Experiments show [24, 40] that the tendency towards Mott physics is stronger in  $\text{Fe}_{1+y}\text{Te}$  than in other parent compounds of FeSCs, suggesting that the magnetic order in  $\text{Fe}_{1+y}\text{Te}$  can be reasonably well understood within the localized scenario by solving the Heisenberg model with exchange interaction extending up to third neighbors [27]. Several groups argued [19, 21, 27, 41] that the ordered up-up-down-down spin configuration is diagonal double stripe. Such an order breaks  $C_4$  lattice rotational symmetry. We argued, based on our analysis of quantum fluctuations in the Heisenberg model with first, second, and third-neighbor exchange, that such a state is unstable, but another up-up-down-down state – the orthogonal double stripe, is stable and is the ground state in some parameter range. This state (which is also called a plaquette state) breaks  $Z_4$  translational symmetry, preserves  $C_4$  symmetry, and does not cause orthorhombic distortion. Also, its structure factor has four equivalent peaks at  $(\pm\pi/2, \pm\pi/2)$ , in agreement with recent neutron scattering studies of  $\text{Fe}_{1+y}\text{Te}$  [22]. An interesting issue that deserves further study is whether  $Z_4$  translational symmetry can be broken before a true ODS spin order sets in, as it happens in other systems [42].

*Acknowledgement.* We acknowledge useful conversations with C. Batista, R. Fernandes, G-W. Chern, M. Graf, B. Lake, A. Nevidomskyy, J. Schmalian, N. Shannon, and I. Zaliznyak. N.B.P. is supported by NSF-DMR-0844115, A.V.C. is supported by NSF-DMR-0906953.



- 
- [1] K. Ishida, Y. Nakai, and H. Hosono, J. Phys. Soc. Japan **78**, 062001 (2009).
- [2] M.D. Johannes and I.I. Mazin, Phys. Rev. B **79**, 220510 (2009).
- [3] J. Paglione and R.L. Greene, Nature Phys. **6**, 645 (2010).
- [4] M.M. Qazilbash, J.J. Hamlin, R.E. Baumbach, L. Zhang, D.J. Singh, M.B. Maple, and D.N. Basov, Nature Physics **5**, 647-650 (2009).
- [5] A.V. Chubukov, Physica C **469**, 640 (2009).
- [6] I.I. Mazin and J. Schmalian, Physica C, 469, 614 (2009).
- [7] V. Stanev, J. Kang, Z. Tesanovic, Phys. Rev. B **78**, 184509 (2008).
- [8] V. Cvetkovic and Z. Tesanovic, Phys. Rev. B **80**, 024512 (2009).
- [9] I. Eremin and A. V. Chubukov, Phys. Rev. B **81**, 024511 (2010).
- [10] D. C. Johnston, Adv. Phys. **59**, 803 (2010).
- [11] P.J. Hirschfeld, M.M. Korshunov, and I.I. Mazin, Rep. Prog. Phys. **74**, 124508 (2011).
- [12] A.V. Chubukov, Annul. Rev. Cond. Mat. Phys. **3**, (2012).
- [13] D.N. Basov and A.V. Chubukov, Nature Physics, **7**, 273 (2011).
- [14] Y. Ran, F. Wang, H. Zhai, A. Vishwanath, and D.-H. Lee, Phys. Rev. B **79**, 014505 (2009).
- [15] R. Fernandes, A.V. Chubukov, I. Eremin, J. Knolle, and J. Schmalian, Phys. Rev. B **85**, 024534 (2012).
- [16] E. Abrahams and Q. Si, J. Phys.: Condens. Matter **23**, 223201 (2011).
- [17] C. Weber and F. Mila, arXiv:1207.0095.
- [18] J.-P. Castellan, S. Rosenkranz, E. A. Goremychkin, D. Y. Chung, I. S. Todorov, M. G. Kanatzidis, I. Eremin, J. Knolle, A. V. Chubukov, S. Maiti, M. R. Norman, F. Weber, H. Claus, T. Guidi, R. I. Bewley, and R. Osborn, Physical Rev. Lett. **107**, 177003 (2011).
- [19] S. Li, *et al.*, C. de la Cruz, Q. Huang, Y. Chen, J. W. Lynn, J-P Hu, Y-L Huang, F-C Hsu, K-W Yeh, M-K Wu, and P. Dai Phys. Rev. B **79**, 054503 (2009).
- [20] T.J. Liu *et al.*, Nature Mater. **9**, 718 (2010).
- [21] O. J. Lipscombe, G. F. Chen, C. Fang, T. G. Perring, D. L. Abernathy, A. D. Christianson, T. Egami, N. Wang, J-P Hu, and P. Dai, Phys. Rev. Lett. **106**, 057004 (2011).
- [22] I. Zalitznyak, *et al.*, Z. Xu, J. Tranquada, G. Gu, A. Tsvelik, M. Stone, Phys. Rev. Lett. **107**, 216403 (2011).
- [23] I. A. Zalitznyak, *et al.*, Z. J. Xu, J. S. Wen, J. M. Tranquada, G. D. Gu, V. Solovyov, V. N. Glazkov, A. I. Zheludev, V. O. Garlea, and M. B. Stone, Phys. Rev. B **85**, 085105 (2012).
- [24] Y. Mizuguchi and Y. Takano, J. Phys. Soc. Jpn. **79**, 102001 (2010).
- [25] Y. Xia, *et al.*, D. Qian, L. Wray, D. Hsieh, G. F. Chen, J. L. Luo, N. L. Wang, and M. Z. Hasan, Phys. Rev. Lett. **103**, 037002 (2009).
- [26] A. Subedi, L. Zhang, D.J. Singh, M.H. Du, Phys. Rev. B **78**, 134514 (2008).
- [27] F. Ma, W. Ji, J. Hu, Z. Lu, and T. Xiang, Phys. Rev. Lett. **102**, 177003 (2009).
- [28] R. Yu, Z. Wang, P. Goswami, A. Nevidomskyy, Q. Si, E. Abrahams, arXiv:1112.4785v1 [cond-mat.str-el]
- [29] H. Hu, B. Xu, W. Liu, N. Hao, Y. Wang, Phys. Rev. B **85**, 144403 (2012).
- [30] J. Zhao, D. Yao, S. Li, T. Hong, Y. Chen, S. Chang, W. Ratcliff, II, J. W. Lyn, H. A. Mook, G.F. Chen, J.L. Luo, N.L. Wang, E.W. Carlson, J. Hu, and P. Dai, Phys. Rev. Lett. **101**, 167203 (2008).
- [31] D. Yao and E.W. Carlson, Phys. Rev. B **78**, 052507 (2008).
- [32] Q. Si and E. Abrahams, Phys. Rev. Lett **101**, 076401 (2008).
- [33] Ari M. Turner, Fa Wang, Ashvin Vishwanath, Phys. Rev. B **80**, 224504 (2009).
- [34] P. Sindzingre, N. Shannon, T. Momoi, arXiv:0907.4163v1; Journal of Physics: Conference Series **200**, 022058 (2010).
- [35] Y-Y. Tai, J-X. Zhu, M. J. Graf, and C. S. Ting, arXiv:12045768v1
- [36] J. Reuther, P. Wölfle, R. Darradi, W. Brenig, M. Arlego, and J. Richter, Phys. Rev. B **83**, 064416 (2011)
- [37] M. Mambrini, A. Lauchli, D. Poilblanc, and F. Mila, Phys. Rev. B. **74**, 144422 (2006)
- [38] P. Chandra and B. Doucot, Phys. Rev. B **38**, 9335 (1988); A. Moreo, E. Dagotto, T. Jolicoeur, and J. Rivera, Phys. Rev. B **42**, 6283 (1990); F. Mila, D. Poilblanc, and C. Bruder, Phys. Rev. B **43**, 7891 (1991); A.V. Chubukov, Phys. Rev. B **44**, 392 (1991).
- [39] see Supplementary Information.
- [40] A. Tamaai, A. Y. Ganin, E. Rozbicki, J. Bacsá, W. Meevasana, P. D. C. King, M. Caffio, R. Schaub, S. Margadonna, K. Prassides, M. J. Rosseinsky, and F. Baumberger, Phys. Rev. Lett. **104**, 097002 (2010).
- [41] C. Fang, B. Xu, P. Dai, T. Xiang, J. Hu, Phys. Rev. B. **85**, 134406 (2012)
- [42] G.-W. Chern, R. M. Fernandes, R. Nandkishore, A. V. Chubukov, arXiv:1203.5776

# Supplemental Material

Samuel Ducatman, Natalia B. Perkins, Andrey Chubukov

Department of Physics, University of Wisconsin-Madison, Madison, WI 53706, USA

In this Supplementary Material we provide details of our analysis of how quantum fluctuations lift accidental nodes in the spin-wave spectra of the sub-set of states selected by quantum fluctuations in the  $J_1$ - $J_2$ - $J_3$  model at  $J_3 > J_2/2$  and  $J_1 = 0$  (i.e., in the  $J_2$ - $J_3$  model with  $J_3 > J_2/2$ ). The Hamiltonian for the model is given by Eq. (1) in the main text. At  $J_1 = 0$  spins on even and odd sites do not interact with each other. It is therefore sufficient to consider only the sub-set made out of spins on, say, even sites.

Classically degenerate ground states are shown in Fig. 2 of the main text. For spins on even sites, any two-sublattice configuration with arbitrary angle  $\gamma$  between spins in  $a$  and  $b$  sublattices is the ground state. Like we said in the text, quantum fluctuations break this degeneracy and select the states at  $\gamma = 0$  or  $\gamma = \pi$  as the only two ground states. The state with  $\gamma = 0$  can be viewed as a spiral state with  $Q_1 = (\pi/2, -\pi/2)$ , and the  $\gamma = \pi$  state corresponds to a spiral with  $Q_2 = (\pi/2, \pi/2)$ . Because only even sites are involved, configurations with  $Q_i$  and  $-Q_i$  are identical.

The classical spectrum of either  $Q_1$  or  $Q_2$  state contains zero modes at corresponding  $Q$ , which must be there by Goldstone theorem, but also contains zero modes at "wrong  $Q$ " (at  $Q_2$  for the  $Q_1$  spiral and vice versa). These last modes are not associated with symmetry breaking (i.e., are "accidental") and must be lifted by quantum fluctuations. In the main text we stated that quantum fluctuations do gap accidental zero modes and studied the consequences. Here we show how this actually happens. For definiteness, we consider  $Q_1$  configuration ( $\gamma = 0$ ).

The lifting of accidental zero modes can be studied within the original two-sublattice picture, with two different bosons describing fluctuations of spins in  $a$  and  $b$  sublattices. It is more convenient, however, to perform a uniform rotation to a local reference frame in which the magnetic order is ferromagnetic and describe the excitation spectrum using just one Holstein-Primakoff boson operator  $a_i$ :

$$\begin{aligned} S_i^z &= S - a_i^\dagger a_i \\ S_i^+ &= (2S - a_i^\dagger a_i)^{\frac{1}{2}} a_i \\ S_i^- &= a_i^\dagger (2S - a_i^\dagger a_i)^{\frac{1}{2}}, \end{aligned} \quad (S.1)$$

As it is customary to spin-wave analysis, we assume that  $S$  is large. Our goal is to obtain the excitation spectrum for  $Q_1$  configuration including terms of order  $1/S$ , which describe quantum fluctuations. Accordingly, we

substitute Eq. (S.1) into Hamiltonian (Eq. (1)) and then expand it to the quartic order in  $a$  field. We obtain

$$H = E_0 + S(H_2 + H_4), \quad (S.2)$$

where  $H_2$  and  $H_4$  are the quadratic and the quartic terms, respectively. In momentum space, we have

$$H_2 = \sum_{\mathbf{k}} \left( A_{\mathbf{k}} a_{\mathbf{k}}^\dagger a_{\mathbf{k}} + \frac{B_{\mathbf{k}}}{2} (a_{\mathbf{k}} a_{-\mathbf{k}} + h.c.) \right), \quad (S.3)$$

where

$$\begin{aligned} A_{\mathbf{k}} &= 4J_3 + 2J_2 \cos(k_x + k_y) \\ B_{\mathbf{k}} &= -2J_3 (\cos(2k_x) + \cos(2k_y)) - 2J_2 \cos(k_x - k_y) \end{aligned} \quad (S.4)$$

and  $\mathbf{k}$  is defined in the first magnetic BZ. The quartic part of the large- $S$  expansion is given by

$$\begin{aligned} H_4 &= \frac{J_2}{8NS} \sum_{\{\mathbf{k}_i\}} \delta \left( \sum_i \mathbf{k}_i \right) \left[ a_{-\mathbf{k}_1}^\dagger a_{\mathbf{k}_2} a_{\mathbf{k}_3} a_{\mathbf{k}_4} \cos(k_{4x} - k_{4y}) \right. \\ &\quad - a_{-\mathbf{k}_1}^\dagger a_{-\mathbf{k}_2}^\dagger a_{\mathbf{k}_3} a_{\mathbf{k}_4} \cos(k_{4x} + k_{4y}) \\ &\quad \left. - 2a_{-\mathbf{k}_1}^\dagger a_{-\mathbf{k}_2}^\dagger a_{\mathbf{k}_3} a_{\mathbf{k}_4} \sin(k_{2x} + k_{4x}) \sin(k_{2y} + k_{4y}) + h.c. \right] \\ &\quad + \frac{J_3}{8NS} \sum_{\{\mathbf{k}_i\}} \delta \left( \sum_i \mathbf{k}_i \right) \left[ a_{-\mathbf{k}_1}^\dagger a_{\mathbf{k}_2} a_{\mathbf{k}_3} a_{\mathbf{k}_4} (\cos 2k_{4x} + \cos 2k_{4y}) \right. \\ &\quad \left. - a_{-\mathbf{k}_1}^\dagger a_{-\mathbf{k}_2}^\dagger a_{\mathbf{k}_3} a_{\mathbf{k}_4} (\cos 2(k_{2y} + k_{4y}) + \cos 2(k_{2x} + k_{4x})) + h.c. \right] \end{aligned} \quad (S.5)$$

The quadratic Hamiltonian  $H_2$  is diagonalized by introducing the Bogoliubov transformation,  $\alpha_{\mathbf{k}} = u_{\mathbf{k}} a_{\mathbf{k}} - v_{\mathbf{k}} a_{-\mathbf{k}}^\dagger$ , where the coherence factors  $u_{\mathbf{k}}$  and  $v_{\mathbf{k}}$  are determined by

$$\begin{aligned} u_{\mathbf{k}} &= \frac{1}{2} \sqrt{\frac{A_{\mathbf{k}} + \Omega_{\mathbf{k}}}{\Omega_{\mathbf{k}}}}, \\ v_{\mathbf{k}} &= -\frac{\text{sign} B_{\mathbf{k}}}{2} \sqrt{\frac{A_{\mathbf{k}} - \Omega_{\mathbf{k}}}{\Omega_{\mathbf{k}}}} \end{aligned}$$

and

$$\Omega_{\mathbf{k}} = S \sqrt{A_{\mathbf{k}}^2 - B_{\mathbf{k}}^2}.$$

The diagonalized Hamiltonian  $H_2$  is given by

$$H_2 = E_2 + \sum_{\mathbf{k}} \Omega_{\mathbf{k}} \alpha_{\mathbf{k}}^\dagger \alpha_{\mathbf{k}}, \quad (S.6)$$

where

$$E_2 = \frac{S}{2} \sum_{\mathbf{k}} (-A_{\mathbf{k}} + \Omega_{\mathbf{k}}) \quad (S.7)$$

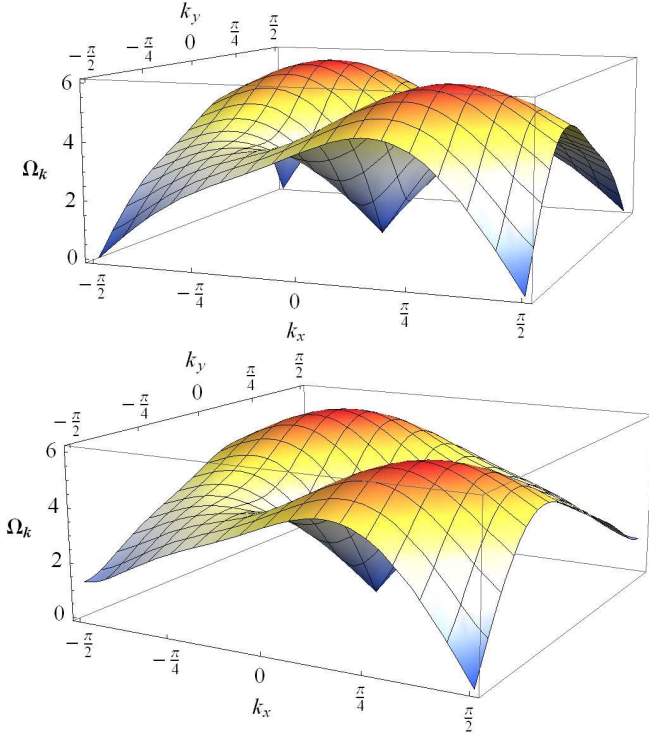


FIG. 3: Excitation spectrum for  $Q_1$  spiral. Top panel: The spectrum of non-interacting bosons, Eq.(S.6). This spectrum contains zero modes at  $\pm(\pi/2, \pi/2)$  and  $\pm(\pi/2, -\pi/2)$ . Bottom panel: the spectrum renormalized by quantum fluctuations to order  $1/S$ . The true Goldstone modes at  $\pm\mathbf{Q}_1 = \pm(\frac{\pi}{2}, -\frac{\pi}{2})$  remain, but the accidental zeroes at  $\pm\mathbf{Q}_2 = \pm(\frac{\pi}{2}, \frac{\pi}{2})$  are removed by quantum fluctuations.

is the contribution to the ground state energy from non-interacting  $a$ -bosons

The spin-wave dispersion of non-interacting bosons is  $\Omega_{\mathbf{k}}$ . At  $\mathbf{k} = \pm\mathbf{Q}_1$  and  $\mathbf{k} = \pm\mathbf{Q}_2$ ,  $A_{Q_{1(2)}} = B_{Q_{1(2)}} = 4J_3 \pm 2J_2$ , where  $+$  and  $-$  signs are for  $Q_1$  and  $Q_2$ , respectively. As a result,  $\Omega_{Q_1} = \Omega_{Q_2} = 0$ . However, as we said, only the zero mode at  $\mathbf{k} = \pm\mathbf{Q}_1$  is the true Goldstone mode, the other one is accidental and must be gapped by quantum fluctuations. To show this, we have to compute  $1/S$  corrections to the spectrum at these points.

The  $1/S$  contribution to  $\Omega_{\mathbf{k}}$  is obtained by evaluating the first-order correction from  $H_4$  what amounts to decoupling of  $H_4$  into the product of two pairs of  $a$ -bosons and replacing one pair by its average value for non-interacting bosons. We first define the averages

$$\begin{aligned} K_{\mathbf{q}} &= \langle a_{\mathbf{q}}^\dagger a_{\mathbf{q}} \rangle = v_{\mathbf{q}}^2, \quad (S.8) \\ L_{\mathbf{q}} &= \langle a_{\mathbf{q}} a_{-\mathbf{q}} \rangle = \langle a_{-\mathbf{q}}^\dagger a_{\mathbf{q}}^\dagger \rangle = u_{\mathbf{q}} v_{\mathbf{q}}. \end{aligned}$$

The decoupled  $H_4$  is

$$\bar{H}_4 = \frac{1}{8NS} \sum_{\mathbf{k}, \mathbf{q}} \left( a_{\mathbf{k}}^\dagger a_{\mathbf{k}} F_1(\mathbf{k}, \mathbf{q}) + \right.$$

$$\left. (a_{\mathbf{k}} a_{-\mathbf{k}} + a_{-\mathbf{k}}^\dagger a_{\mathbf{k}}^\dagger) \frac{F_2(\mathbf{k}, \mathbf{q})}{2} \right), \quad (S.9)$$

where

$$\begin{aligned} F_1(\mathbf{k}, \mathbf{q}) &= -2J_3 \left( 4K_{\mathbf{q}} (\cos^2(k_x - q_x) + \cos^2(k_y - q_y)) \right. \\ &\quad \left. - L_{\mathbf{q}} (2(\cos 2q_x + \cos 2q_y) + \cos 2k_x + \cos 2k_y) \right) \\ &\quad - 2J_2 \left( K_{\mathbf{q}} (4 \sin(k_x - q_x) \sin(k_y - q_y)) \right. \\ &\quad \left. + 2 \cos(k_x + k_y) + 2 \cos(q_x + q_y) \right) \\ &\quad \left. - L_{\mathbf{q}} (2 \cos(q_x - q_y) + \cos(k_x - k_y)) \right), \\ F_2(\mathbf{k}, \mathbf{q}) &= 2J_3 \left( K_{\mathbf{q}} (\cos 2q_x + \cos 2q_y) \right. \\ &\quad \left. + 2(\cos 2k_x + \cos 2k_y) \right) \\ &\quad - 2L_{\mathbf{q}} (\cos 2(k_x - q_x) + \cos 2(k_y - q_y)) \\ &\quad + 2J_2 \left( K_{\mathbf{q}} (\cos(q_x - q_y) + 2 \cos(k_x - k_y)) \right. \\ &\quad \left. + L_{\mathbf{q}} (-4 \sin(k_x - q_x) \sin(k_y - q_y) \right. \\ &\quad \left. - \cos(k_x + k_y) - \cos(q_x + q_y)) \right) \end{aligned}$$

Combining the decoupled  $H_4$  with  $H_2$  expressed in terms of original  $a$ -operators we obtain

$$\begin{aligned} H_2 + \bar{H}_4 &= \sum_{\mathbf{k}} \left[ \left( A_{\mathbf{k}} + \frac{A_{\mathbf{k}}^{(4)}}{S} \right) a_{\mathbf{k}}^\dagger a_{\mathbf{k}} + \right. \\ &\quad \left. \frac{1}{2} \left( B_{\mathbf{k}} + \frac{B_{\mathbf{k}}^{(4)}}{S} \right) (a_{\mathbf{k}} a_{-\mathbf{k}} + h.c.) \right], \quad (S.10) \end{aligned}$$

where

$$\begin{aligned} A_{\mathbf{k}}^{(4)} &= \frac{1}{8N} \sum_{\mathbf{q}} F_1(\mathbf{k}, \mathbf{q}), \\ B_{\mathbf{k}}^{(4)} &= \frac{1}{8N} \sum_{\mathbf{q}} F_2(\mathbf{k}, \mathbf{q}) \end{aligned}$$

At  $\mathbf{k} = \mathbf{Q}_1$  and  $\mathbf{k} = \mathbf{Q}_2$  we have

$$\begin{aligned} A_{Q_{1(2)}}^{(4)} &= \frac{-1}{4N} \sum_{\mathbf{q}} J_3 \left( 4K_{\mathbf{q}} (\sin^2(q_x) + \sin^2(q_y)) \right. \\ &\quad \left. - L_{\mathbf{q}} (2(\cos 2q_x + \cos 2q_y) - 2) \right) \\ &\quad + J_2 \left( K_{\mathbf{q}} (\mp 4 \cos(q_x) \cos(q_y)) \right. \\ &\quad \left. \pm 2 + 2 \cos(q_x + q_y) \right) \\ &\quad \left. - L_{\mathbf{q}} (2 \cos(q_x - q_y) \mp 2) \right), \\ B_{Q_{1(2)}}^{(4)} &= \frac{1}{4N} \sum_{\mathbf{q}} J_3 \left( K_{\mathbf{q}} (\cos 2q_x + \cos 2q_y - 4) \right. \\ &\quad \left. + 2L_{\mathbf{q}} (\cos 2q_x + \cos 2q_y) \right) \\ &\quad + J_2 \left( K_{\mathbf{q}} (\cos(q_x - q_y) \mp 2) \right. \\ &\quad \left. + L_{\mathbf{q}} (\pm 4 \cos(q_x) \cos(q_y) \right. \\ &\quad \left. \mp 1 - \cos(q_x + q_y)) \right), \end{aligned}$$

where the upper and the lower signs correspond to  $\mathbf{Q}_1$  and  $\mathbf{Q}_2$  vectors, respectively. One can easily make sure that  $A_{\mathbf{Q}_1}^{(4)} = B_{\mathbf{Q}_1}^{(4)}$ , but  $A_{\mathbf{Q}_2}^{(4)} \neq B_{\mathbf{Q}_2}^{(4)}$ . Thus, when  $1/S$  corrections are included, the spectrum at  $\mathbf{Q}_1$  remains gapless, as it should be, but at  $\mathbf{Q}_2$  the gap opens up, i.e., quantum fluctuations lift the accidental degeneracy at the "wrong  $Q$ ". We computed the renormalized spectrum

for all  $\mathbf{k}$  and show the results in Fig.3. The renormalized spectrum, shown in the bottom panel, clearly has a gap at  $\pm(\pi/2, \pi/2)$ , where the spectrum of non-interacting bosons (top panel) has zero modes. We verified that the same effect (lifting of accidental nodes) holds if we use biquadratic spin interaction instead of quantum fluctuations.